IEEE Access
Multidisciplinary | Rapid Review | Open Access Journal

Received August 13, 2019, accepted September 5, 2019, date of publication September 16, 2019, date of current version October 3, 2019.

Digital Object Identifier 10.1109/ACCESS.2019.2941593

Enhancing Resilience Level of Power Distribution Systems Using Proactive Operational Actions

BABAK TAHERI[1], AMIR SAFDARIAN[1], (Member, IEEE), MOEIN MOEINI-AGHTAIE[2], (Member, IEEE), AND MATTI LEHTONEN[3]

[1]Center of Excellence in Power System Control and Management, Electrical Engineering Department, Sharif University of Technology, Tehran 11365-11155, Iran
[2]Department of Energy Engineering, Sharif University of Technology, Tehran 11365-11155, Iran
[3]Department of Electrical Engineering and Automation, Aalto University, Espoo, Finland

Corresponding author: Amir Safdarian (safdarian@sharif.edu)

ABSTRACT Growing widespread outages in power systems caused by natural disasters have highlighted the necessity of applying defensive approaches with the goal of prompt service restoration. In this context, this paper proposes a stochastic model with the goal of optimally using proactive operational actions before the upcoming disturbance hits. The actions considered in this study include network reconfiguration and crew prepositioning. To take the effective actions, the model simulates probable damages caused by the events via a set of scenarios generated by Monte Carlo simulation method. The proposed model aims at minimizing the expected load curtailment caused by the event over the scenarios. To calculate the amount of load curtailments, potential post-disturbance actions are also considered in the model. The model is mathematically formulated in mixed integer linear programming (MILP) fashion which can be easily solved via available software packages. A standard distribution system with a realistic set of data is employed to validate the effectiveness of the proposed model.

INDEX TERMS Power distribution system, system resilience, natural disaster, optimal crew dispatching, optimal crew prepositioning.

NOMENCLATURE

SETS AND INDICES

m, n	Indices of buses.
i, j	Indices for lines, depots and staging locations.
dp	Index of the depot.
st	Index of staging locations.
cr	Set of crew teams.
l	Index of lines.
t	Index of time for the pre-disturbance stage.
t'	Index of time for the post-disturbance stage.
s	Index of scenarios.
N_t	The total number of t.
ψ_m	Set of buses connected to bus m by a line.
S	Set of scenarios.

PARAMETERS

$P^D_{t,m}, Q^D_{t,m}$	Active and reactive power demand at bus m at time t.
cap_l	The capacity of line l.
x_i^{MS}	Binary parameter equals to 1 if point i has a manual switch.
x_i^{RCS}	Binary parameter equals to 1 if point i has a remote-controlled switch.
EP	Event predictability.
M	Satisfactorily large positive number.
r_l, x_l	Resistance/ reactance of line l.
$TT_{i,j}$	Travel time between point i and j.
ST_i	The time needed to change the status of the switch at point i.
RST	Remote switching time.
$TCF_{i,j}$	Traffic congestion factor.
Pr^s	Probability of scenario s.
ω_m	Weight factor for load at bus m.
$\Delta t'$	Time step.
d_l^s	Binary parameter equals to 0 if line l is damaged at scenario s.
$\overline{V}$, $\underline{V}$	Maximum/minimum allowed voltage.
S	Maximum apparent power of the main grid.
$\overline{P_m^{DG}}, \underline{P_m^{DG}}$	Maximum/minimum active power output of DG at bus m.
$\overline{Q_m^{DG}}, \underline{Q_m^{DG}}$	Maximum/minimum reactive power output of DG at bus m.

The associate editor coordinating the review of this manuscript and approving it for publication was Baoping Cai.

$\overline{P^{PV}_{t,m}}$	Maximum active power output of photovoltaic at bus m at time t.
$\overline{P^{WT}_{t,m}}$	Maximum active power output of the wind turbine at bus m at time t.

VARIABLES

$P^{f}_{t,l}$, $Q^{f}_{t,l}$	Active/reactive power flow of line l at time t.
$P^{LC}_{t',m}$, $Q^{LC}_{t',m}$	Active/reactive load curtailment at bus m at time t'.
$P^{DG}_{t,m}$, $Q^{DG}_{t,m}$	Output active/reactive power of DG at bus m at time t.
$P^{WT}_{t,m}$, $Q^{WT}_{t,m}$	Output active/reactive power of wind turbine at bus m at time t.
$P^{PV}_{t,m}$, $Q^{PV}_{t,m}$	Output active/reactive power of photovoltaic at bus m at time t.
$time^{cr}_{j}$	Arrival time of crew cr at point j.
$Disp^{cr}_{i,j}$	Binary variable equals to 1 if crew cr is dispatched from i to j.
$\alpha_{t,l}$	Binary variable equals to 1 if the switch of line l is closed at time t.
$\vartheta_{t',l}$	Binary variable equals 1 if line l is in a serviceable state at the time t'.
$\Phi_{t,l}$	Binary variable equals to 1 if the status of the switch of line l changes at time t.
$\beta_{t,m}$	Binary variable equals to 1 if DG at bus m at time t is scheduled.
$V_{t,m}$	Voltage magnitude of bus m at time t.
$\gamma_{m,n,t}$	Binary variable equals to 1 if bus n is the parent of bus m.
pX	Post-disturbance version of variable/ parameter X.

I. INTRODUCTION

Recently, natural calamities have significantly affected the electricity supply continuity all over the world [1]. As an example, hurricane sandy after hitting the eastern shore of the United States left nearly 7.5 million customers without electricity [2], [3]. Hence, boosting the resilience of power systems to deal with such events has been highlighted more than before. Due to the fact that power distribution systems are the most vulnerable part of power systems, more attention ought to be devoted to this sector of power systems [4]. The word ''resilience'' meaning the ''act of rebounding'' stems from the Latin word ''resilire,'' which means ''the ability to spring back or rebound'' [5]. According to [6], resilience engineering ''uses the insights from research on failures in complex systems, including organizational contributors to risk, and the factors that affect human performance to provide systems engineering tools to manage risks proactively.'' Furthermore, a comprehensive definition for the infrastructure resilience is offered by the National Infrastructure Advisory Council (NIAC) as ''the ability to reduce the magnitude and/or duration of disruptive events. The effectiveness of a resilient infrastructure or enterprise depends upon its ability to anticipate, absorb, adapt to, and/or rapidly recover from a potentially disruptive event'' [7]. Also, according to the UK Energy Research Center, resilience is ''the capacity of an energy system to tolerate disturbance and to continue to deliver affordable energy services to consumers. A resilient energy system can speedily recover from shocks and can provide alternative means of satisfying energy service needs in the event of changed external circumstances'' [8]. According to Presidential Policy Directive 21, resilience is ''the ability to prepare for and adapt to changing conditions and withstand and recover rapidly from disruption'' [9]. Accordingly, contemplating all the aforementioned definitions, a resilient system should comprise the following characteristics: avoidance, survival, and recovery. In the literature, improving resilience of power distribution systems to cope with disastrous events has been studied from distinctive perceptions. Also, various metrics such as availability-based metrics for evaluating resilience engineering have been studied in the literature [10], wherein using the introduced metric, a new dynamic-Bayesian-network-based methodology has been proposed for evaluating the resilience value of engineering systems.

In some studies, hardening of distribution system components has been proposed to deal with natural hazards [11]–[13]. The study reported in [13], has proposed a two-stage stochastic MILP model to design a resilient distribution system. The first stage involves deploying resilience-oriented design of resources (e.g., automatic switches and back-up distributed generations (DGs)) and hardening distribution lines. In the second stage, system operation cost during the extreme weather event is evaluated [14], [15]. Also, a new metric for resilience measure has been introduced in [16] thereby a comprehensive approach for resilient system design under internal deterioration and external distress has been proposed. Then, by using a combinatorial analysis, the relationship between system resilience and the damage is attained. Although infrastructure hardening could boost the strength of power distribution systems in dealing with disastrous events, they call for considerable investments from utility companies. Some other studies have proposed operational strategies to enhance power distribution resilience. In some studies, it has been proposed to divide distribution networks into self-sufficient microgrids after the occurrence of the event [17]–[19]. Authors in [19] have proposed a multi-microgrid formation after the occurrence of a major fault due to a natural disaster with the aid of available remote controlled switches (RCSs) and DGs to pick up critical loads. The proposed method was formulated as a MILP problem. In [20], a MILP model has been proposed for post-fault multi-time step service restoration under cold load pickup conditions in presence of RCSs, DGs, and energy storage (ESs) systems. In [21], a two-stage stochastic model has been proposed for resilience enhancement of power distribution systems via taking advantages of mobile ESs.

Furthermore, considering load balancing as a constraint in the study, [22] has proposed a reinforcement learning-oriented (i.e., wolf pack algorithm) agent-based restoration strategy for smart grids. Besides the reviewed works, some studies have emphasized preventive actions that should be adopted prior to the occurrence of approaching disastrous events [23]–[26]. Authors in [23] have accomplished robust pre-disturbance scheduling of microgrids with the aim of minimizing the cost of high impact low probability events by the implementation of column-and-constraint generation (C&CG) algorithm. The study in [27] has presented a new algorithm to find the number and location of depots at the pre-disturbance stage to manage the available resources right after stricken of the event. The authors in [28] have offered a two-stage stochastic model to minimize restoration costs via allocating available distributed energy resources proactively in advance of a hurricane. Also, pre-positioning and real-time allocation of mobile emergency generators have been studied in [29] and [30]. Authors in [31] and [32] have presented proactive scheduling for distribution networks by identifying vulnerable lines and tripping them out intentionally prior to the occurrence of approaching extreme weather events. The repair procedure of damaged components after the occurrence of a catastrophic event has been studied in [33], [34]. Since repair actions are usually time expensive, advantages of available sources, RCSs, and manual switches (MSs) were taken before starting the repair process.

In order to move toward more resilient systems, this paper proposes a model to optimally employ available resources in dealing with predictable natural disasters. In this regard, the model reconfigures the network to obtain a more resilient configuration considering the likely consequences of the upcoming disturbance. In addition, to expedite the expected post-disturbance actions, available maneuver crew teams are prepositioned in proper locations. Needless to mention, taking the proper decisions associated with network reconfiguration and crew prepositioning calls for simulating likely consequences of the approaching event. To do so, the Monte Carlo simulation method is employed for generating likely damage scenarios using the failure probability of power distribution lines extracted from fragility curves [35]. The proposed model is to minimize the expected load curtailment caused by the event over the scenarios. To calculate the amount of load curtailments, potential post-disturbance actions are also considered in the model. Needless to mention, contemplating all the scenarios, the model makes a unique decision for all pre-disturbance actions. The model is mathematically formulated in mixed integer linear programming (MILP) fashion which can be easily solved via available software packages. The proposed model is applied to a test bed, and the simulation results reveal its significant performance.

The rest of the paper is organized as follows. Section II presents the problem description and methodology. Section III describes the mathematical formulation of the proposed model. The case study and simulation results are presented in Section IV. Section V concludes the study.

II. PROBLEM DESCRIPTION AND METHODOLOGY

In many occasions, disturbances cannot be predicted in advance. An earthquake is an example of such disturbances. Needless to mention, it is inevitable to focus on the optimal scheduling of post-disturbance actions in dealing with such disturbances. There are however some disturbances such as severe weather conditions, floods, and thunderstorms which can be predicted in advance. In these occasions, it makes sense to focus on both pre-disturbance and post-disturbance actions to mitigate the consequences of the event. To do so, this paper proposes a model to optimize the schedule of pre-disturbance actions. There are a variety of actions a system operator can take before an event. The proposed model however mainly focuses on network reconfiguration and crew prepositioning. Synonymously, the model aims at extracting the best possible configuration of the network prior to the approaching disturbance and prepositioning crew teams for speeding up likely post-disturbance operations. It is clear that likely damages of the upcoming event have a stochastic nature. So, the model is a stochastic one wherein uncertainty associated with potential damages is captured via a set of likely scenarios. Here, a scenario represents the operating status of network lines during and after the event. In order to sample damage scenarios, fragility curves of power distribution lines are used in this paper. The fragility curves together with the severity of the approaching event are employed to determine the failure probability of lines under disturbance excitation. Interested readers are referred to [24], [31], [32], [36] where estimating failure probability of system components based on the intensity of natural disasters and their fragility curves have been extensively discussed. Also, using dynamic Bayesian networks in the study, [37] has proposed a new hybrid physics-model-based and data-driven methodology for remaining useful life estimation of structure systems, wherein the value of remaining useful life can be updated using the expert knowledge or sensor data as input values to the estimation model. Failure probabilities of the lines are fed to the Monte Carlo simulation method as input data to generate likely scenarios. It is worthwhile to note that the accuracy of the results increases as the number of generated scenarios grows. However, computational complexity is a barrier which forces scenario-based stochastic models to establish a tradeoff between accuracy and complexity. To alleviate concerns on computational complexity, a scenario reduction approach is implemented in this paper. To ensure that the reduced number of scenarios does not jeopardize the accuracy of the final results, solution stability test is applied here.

Considering the mentioned assumptions and methods, the model is formulated in the next section to minimize the expected load curtailment induced by the disturbance over all generated scenarios. To adhere network operational constraints, power flow equations are considered in the model.

To keep the model simple enough to be solved in available software packages, it is developed in MILP fashion.

The model is fed by network technical data, geographical information of the system components like manual switches, crew teams, and fault locations, and the time the disturbance hits and line damages occur in different scenarios as input data. It then provides an optimal schedule of actions before the disturbance hits the system. It is expected that using the proposed model, not only less load curtailment is caused by a disastrous event but also due to the prepositioned crews, curtailed loads can be restored promptly.

III. MATHEMATICAL FORMULATION

As mentioned before, system operator optimizes system resources once disturbance consequences are forecasted and the set of likely scenarios for post-disturbance system status are generated. This can be done via solving an optimization problem with the aim to minimize the expected post-disturbance load curtailment over all scenarios considering their priorities as follows.

$$Min \sum_{s} \sum_{t'} \sum_{m} Pr^{s}.\omega_{m}.P^{LC}_{s,t',m}.\Delta t' \tag{1}$$

According to the above relation, different priorities can be considered for loads hosted by different buses. It is worthwhile to note that though different objectives like system operation cost and crew fuel cost can be considered too, it does not make a big deal to slightly increase network losses to enhance system resilience in dealing with low probability events. This objective is subject to some technical constraints which are described here. Active and reactive power balance equations at each bus in each time period are as follows.

$$P^{D}_{t,m} - P^{PV}_{t,m} - P^{WT}_{t,m} - P^{DG}_{t,m} - \sum_{l,to=m} P^{f}_{t,l} + \sum_{l,from=m} P^{f}_{t,l} = 0, \quad \forall t, m > 1 \tag{2}$$

$$Q^{D}_{t,m} - Q^{PV}_{t,m} - Q^{WT}_{t,m} - Q^{DG}_{t,m} - \sum_{l,to=m} Q^{f}_{t,l} + \sum_{l,from=m} Q^{f}_{t,l} = 0, \quad \forall t, m > 1 \tag{3}$$

The following expressions adhere to the power flow equations.

$$V_{t,n} - V_{t,m} + \frac{r_l.P^{f}_{t,l} + x_l.Q^{f}_{t,l}}{V_{t,1}} \geq \left(\alpha_{t,l} - 1\right) M, \quad \forall t, l \tag{4}$$

$$V_{t,n} - V_{t,m} + \frac{r_l.P^{f}_{t,l} + x_l.Q^{f}_{t,l}}{V_{t,1}} \leq \left(1 - \alpha_{t,l}\right) M, \quad \forall t, l \tag{5}$$

The expressions addressed in (4) and (5) are based on the linear AC power flow model proposed in [38], i.e., Dist-Flow model. It is worthwhile to mention that the model has been successfully applied in several articles [38]–[40]. In the model, the constraints can be relaxed via the big-M method if the associated line is in open state [32].

In the following, (6) is to guarantee that capacity limit of lines is considered. (7) implies that the voltage magnitude at all buses is within the allowed range. Similarly, (8) guarantees that capacity limit of the substation is considered.

$$-\alpha_{t,l} cap_l \leq P^{f}_{t,l} \leq \alpha_{t,l} cap_l, \quad \forall t, l \tag{6}$$

$$\underline{V} \leq V_{t,m} \leq \overline{V}, \quad \forall t, m \tag{7}$$

$$\left(\sum_{l,from=1} P^{f}_{t,l}\right)^2 + \left(\sum_{l,from=1} Q^{f}_{t,l}\right)^2 \leq S^2, \quad \forall t, l \tag{8}$$

To preserve linearity of the model, (8) is linearized using the special-ordered-sets-of- type 2 (SOS2) method presented in [41]. The set of constraints in (9)–(12) model the limits on the output power of DGs, PVs, and WTs, respectively. Note that the PVs and WTs are assumed to be P-Q sources with a constant power factor. Needless to mention, the limit of PVs and WTs is a time-varying parameter depending on environmental parameters such as wind speed and solar irradiation.

$$\beta_{t,m}.\underline{P^{DG}_{m}} \leq P^{DG}_{t,m} \leq \beta_{t,m}.\overline{P^{DG}_{m}} \quad \forall t, m \tag{9}$$

$$\beta_{t,m}.\underline{Q^{DG}_{m}} \leq Q^{DG}_{t,m} \leq \beta_{t,m}.\overline{Q^{DG}_{m}}, \quad \forall t, m \tag{10}$$

$$0 \leq P^{PV}_{t,m} \leq \overline{P^{PV}_{t,m}}, \quad \forall t, m \tag{11}$$

$$0 \leq P^{WT}_{t,m} \leq \overline{P^{WT}_{t,m}}, \quad \forall t, m \tag{12}$$

The set of constraints in (13)−(15) are considered to ensure the radial configuration of the network. These constraints are borrowed from the spanning tree method explained in [42].

$$\gamma_{m,n,t} + \gamma_{n,m,t} = \alpha_{t,l}, \quad \forall l \in (m, n), \; n \in \psi_m t = EP \tag{13}$$

$$\sum_{n \in \psi_m} \gamma_{m,n,t} \leq 1, \quad \forall n \in \psi_m, \; t = EP \tag{14}$$

$$\gamma_{1,n,t} = 0, \quad \forall n \in \psi_{root}, \; t = EP \tag{15}$$

The following constraint is to limit the number of times that the status of a switch is changed.

$$\sum_{t} \Phi_{t,l} \leq 1, \quad \forall l \tag{16}$$

In the above expression, $\Phi_{t,l}$ takes 1 if the status of the associated switch is changed at time t. The changes in the status are detected via the following expressions.

$$-\Phi_{t,l} \leq \alpha_{t,l} - \alpha_{t-1,l} \leq \Phi_{t,l}, \quad \forall t, l \tag{17}$$

$$\Phi_{t,l} \leq \alpha_{t,l} + \alpha_{t-1,l} \leq 2 - \Phi_{t,l}, \quad \forall t, l \tag{18}$$

The arrival time of crews to the location of point j is calculated in (19) and (20) as follows.

$$time^{cr}_{j} \geq time^{cr}_{i} + TT_{i,j} + ST_{i} - \left(1 - Disp^{cr}_{i,j}\right) M, \quad \forall i, j, cr \tag{19}$$

$$time^{cr}_{j} \leq time^{cr}_{i} + TT_{i,j} + ST_{i} + \left(1 - Disp^{cr}_{i,j}\right) M, \quad \forall i, j, cr \tag{20}$$

In the above expressions, the arrival time to point j is equal to the arrival time to point i, the time needed for traveling

between the two points, and the time needed for changing the status of the switch at point i. The big-M method is used to exclude the constraints associated with the paths which are not traveled by the crew teams [33].

The following constraints are considered to model the logical actions taken by crew teams.

$$\sum_{cr}\sum_{i} Disp^{cr}_{i,l} = \sum_{t} \Phi_{t,l} \quad \forall l \in x^{MS}_{l} \tag{21}$$

$$\sum_{i} Disp^{cr}_{dp,i} = 1, \quad \forall cr \tag{22}$$

$$\sum_{st}\sum_{i} Disp^{cr}_{i,st} = 1, \quad \forall cr \tag{23}$$

$$\sum_{j} Disp^{cr}_{st,j} = 0, \quad \forall cr, st \tag{24}$$

$$time^{cr}_{st} \leq EP, \quad \forall cr, st \tag{25}$$

$$\sum_{i} Disp^{cr}_{i,l} - \sum_{j} Disp^{cr}_{l,j} = 0, \quad \forall cr, l \in x^{MS}_{l} \tag{26}$$

$$\sum_{cr}\sum_{i} Disp^{cr}_{i,l} \leq 1, \quad \forall l \in x^{MS}_{l} \tag{27}$$

$$\sum_{t} t.\Phi_{t,l} \geq \sum_{cr} \left(time^{cr}_{l} + ST_{l} \sum_{i} Disp^{cr}_{i,l}\right), \quad \forall l \in x^{MS}_{l} \tag{28}$$

$$\sum_{t} t.\Phi_{t,l} \leq \sum_{cr} \left(time^{cr}_{l} + ST_{l} \sum_{i} Disp^{cr}_{i,l}\right) + 1 - \epsilon, \quad \forall l \in x^{MS}_{l} \tag{29}$$

$$0 \leq time^{cr}_{j} \leq M \sum_{i} Disp^{cr}_{i,j}, \quad \forall cr, j \tag{30}$$

$$\sum_{i} Disp^{cr}_{i,j} - \sum_{i} Disp^{cr}_{j,i} \geq 0, \quad \forall cr, j/\{dp\} \tag{31}$$

$$\sum_{cr}\sum_{i} Disp^{cr}_{i,l} = 0, \quad \forall cr, l \in x^{RCS}_{l} \tag{32}$$

In the above, (21) guarantees that a crew team is dispatched to a switch location only if changing status of the switch is required. (22) implies that each crew is initially dispatched from the depot. The set of constraints (23)–(25) ensure that all crew teams are finally at one of the staging locations before the approaching disturbance hits. (26) indicates that a crew leaves a switch location only after changing the status of the switch. (27) implies that only one crew can be dispatched to the location of each switch. (28), (29), and (30) are used for determining the time when the status of a switch changes. (31) guarantees that a crew team can leave point i only if they have been previously dispatched to the location. (32) indicates that crew teams must not be dispatched to the location of RCSs since their status can be changed remotely.

The actions taken by the system operator before the event are directly related to the event predictability (EP). In other words, the operator may take several actions if there is enough time and may take just some high priority actions if the time to event is tight. This time limit for RCSs is mathematically formulated as follows.

$$\sum_{t} t.\Phi_{t,l} \geq RST, \quad \forall l \in x^{RCS}_{l} \tag{33}$$

$$\sum_{t} t.\Phi_{t,l} \leq EP, \quad \forall l \in x^{RCS}_{l} \tag{34}$$

The above-mentioned expressions are related to actions taken in the pre-disturbance situation. Here, formulations related to actions after the disturbance are expressed in detail. To avoid unnecessary repetition, equations (7) − (21), (26) − (32) are lumped in (35) where t is substituted by $t^{'}$, and the equations are written for all scenarios (s).

$$(7)-(21),(26)-(32), \quad \forall s, t^{'} \tag{35}$$

$$pP^{D}_{t^{'},m} - P^{LC}_{s,t^{'},m} - pP^{PV}_{s,t^{'},m} - pP^{WT}_{s,t^{'},m} - pP^{DG}_{s,t^{'},m} - \sum_{l,to=m} pP^{f}_{s,t^{'},l} + \sum_{l,from=m} pP^{f}_{s,t^{'},l} = 0, \quad \forall s, t^{'}, m \tag{36}$$

$$pQ^{D}_{t^{'},m} - Q^{LC}_{s,t^{'},m} - pQ^{PV}_{s,t^{'},m} - pQ^{WT}_{s,t^{'},m} - pQ^{DG}_{s,t^{'},m} - \sum_{l,to=m} pQ^{f}_{s,t^{'},l} + \sum_{l,from=m} pQ^{f}_{s,t^{'},l} = 0, \quad \forall s, t^{'}, m \tag{37}$$

$$0 \leq P^{LC}_{s,t^{'},m} \leq pP^{D}_{t^{'},m}, \quad \forall s, t^{'}, m > 1 \tag{38}$$

$$Q^{LC}_{s,t^{'},m} = P^{LC}_{s,t^{'},m} \frac{pQ^{D}_{t^{'},m}}{pP^{D}_{t^{'},m}}, \quad \forall s, t^{'}, m > 1 \tag{39}$$

$$\vartheta^{s}_{t^{'},l} = p\alpha_{s,t^{'},l}.d^{s}_{l}, \quad \forall s, t^{'}, l \tag{40}$$

$$pV_{s,t^{'},n} - pV_{s,t^{'},m} + \frac{r_l.pP^{f}_{s,t^{'},l} + x_l.pQ^{f}_{s,t^{'},l}}{V_1} \geq \left(\vartheta^{s}_{t^{'},l} - 1\right)M, \quad \forall s, t^{'}, l \tag{41}$$

$$pV_{s,t^{'},n} - pV_{s,t^{'},m} + \frac{r_l.pP^{f}_{s,t^{'},l} + x_l.pQ^{f}_{s,t^{'},l}}{V_1} \leq \left(1 - \vartheta^{s}_{t^{'},l}\right)M, \quad \forall s, t^{'}, l \tag{42}$$

$$-\vartheta^{s}_{t^{'},l} cap_l \leq pP^{f}_{s,t^{'},l} \leq \vartheta^{s}_{t^{'},l} cap_l, \quad \forall s, t^{'}, l \tag{43}$$

In the above, (36) and (37) assure the active and reactive power balance at each bus, respectively. It is worthwhile to note that difference between the power balance equations before and after the event goes back to the fact that load curtailment might be inevitable after the event. (38) ensures that load curtailment in each bus does not exceed the total load connected to that bus. (39) is to ensure that the power factor of the load remains the same after the load curtailment. (40) indicates the status of network lines after the event hits the system. (41) and (42) represent linear AC power flow expressions. (43) ensures that the power flowing through lines

is within acceptable limits. The timing of actions taken by crew teams after the event hits the system is calculated as follows.

$$ptime^{cr}_{s,j} \geq ptime^{cr}_{s,i} + TCF_{i,j} \times TT_{i,j} + ST_i - \left(1 - pDisp^{cr}_{s,i,j}\right) M, \quad \forall i, j, cr \tag{44}$$

$$ptime^{cr}_{s,j} \leq ptime^{cr}_{s,i} + TCF_{i,j} \times TT_{i,j} + ST_i - \left(1 - pDisp^{cr}_{s,i,j}\right) M, \quad \forall i, j, cr \tag{45}$$

Equations presented in (44) and (45) represent the time needed for crew teams to take the j^{th} action. (46) guarantees that once the event is finished, crews start their travel from the staging locations where they moved to before the occurrence of the hazard. In addition, (47) is considered for coupling the status of switches in pre- and post-disturbance stages. (48) indicates that once a crew team moves to the location of a switch, the status of the switch should be changed. Finally, (49) guarantees that in each scenario, all of the crew teams should be moved to the depot location after performing the scheduled actions.

$$\sum_i Disp^{cr}_{i,st} - \sum_j pDisp^{cr}_{s,st,j} \geq 0, \quad \forall cr, st \tag{46}$$

$$p\alpha_{s,t',l} = \alpha_{t,l}, \quad \forall l, s, t = N_t, t' = 0 \tag{47}$$

$$\sum_{cr}\sum_i pDisp^{cr}_{s,i,l} = \sum_{t'} p\Phi_{s,t',l}, \quad \forall s, l \in x^{MS}_l \tag{48}$$

$$\sum_{dp}\sum_i pDisp^{cr}_{s,i,dp} = 1, \quad \forall cr, s \tag{49}$$

The set of constraints in (50) − (52) guarantee the radial configuration of the network in the post-disturbance stage.

$$p\gamma_{s,m,n,t'} + p\gamma_{s,n,m,t'} = \vartheta^{s}_{t',l}, \quad \forall s, t', l \in (m,n), n \in \psi_m \tag{50}$$

$$\sum_{n \in \psi_m} p\gamma_{s,m,n,t'} \leq 1, \quad \forall s, m, t', n \in \psi_m \tag{51}$$

$$p\gamma_{s,1,n,t'} = 0, \quad \forall s, t', n \in \psi_{root} \tag{52}$$

The scheduling problem established in the above is in MILP format that can be solved using commercial software packages. The optimal decisions from this optimization problem comprise the pre-disturbance configuration of the system, switching sequence of the switches, the output power of available sources, and prepositioned locations of the crew teams. It should be noted that the developed MILP model is solved by the CPLEX solver in GAMS environment. It is worthwhile to mention that the solver uses a Branch and Bound algorithm (with cuts) and supports specially ordered set variables SOS1, SOS2 as well as semi-continuous and semi-integer variables [43]. The algorithm is an enumerative method which solves MILP problems by relaxing the constraints and using the state-space search. Interested readers are referred to [44] wherein the method is investigated in more details.

IV. NUMERICAL RESULTS

The proposed model is implemented on a 47-bus power distribution system with a realistic set of data as shown in Fig. 1. Parameters of the network are taken from [45]. Fig. 2 illustrates the load profile of the test system. Five dispatchable DGs are considered in the system. The data related to these units are given in Table 1. In addition, a PV unit is hosted by Bus 20. Moreover, three WT units are assumed to be installed at Buses 26, 33, and 37. The output powers of the PVs and WTs during a typical day are shown in Figs. 3 and 4, respectively [45]. As can be seen in Fig. 1, two RCSs are installed on Lines 26 and 43. It is assumed that the event happens at 1 PM. It should be noted that the time step (i.e., $\Delta t'$) is considered to be 5 minutes in the studies. According to the historical data, mainly the occurrence of natural calamities deteriorates traffic congestion problems [46]. These problems mainly occur as a consequence of the severity of the event, which can lead to unexpected broken roads obstructed by external objects like broken trees and damaged cars. In addition, during the extreme events, some people

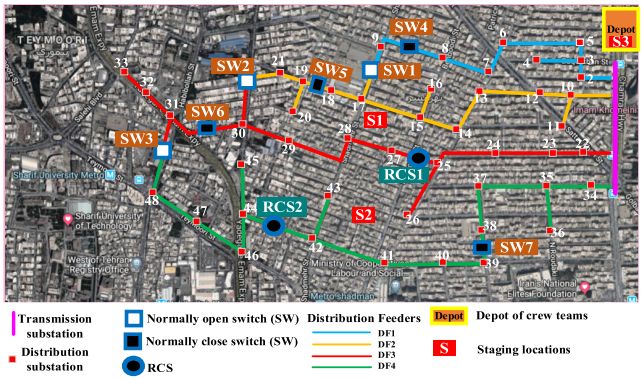

FIGURE 1. Test system under study.

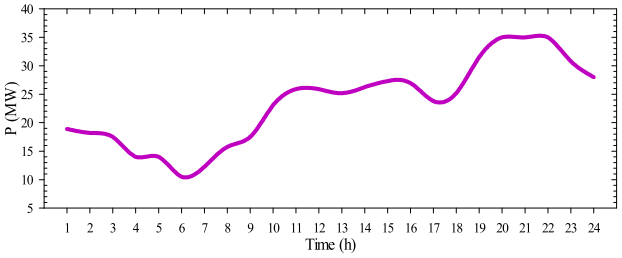

FIGURE 2. Load profile of customers [45].

TABLE 1. Distributed generation units locations and ratings.

DGs	BUS	$\overline{P^{DG}_m}$ (MW)	$\underline{P^{DG}_m}$ (MW)	$\overline{Q^{DG}_m}$ (MVar)	$\underline{Q^{DG}_m}$ (MVar)
DG1	9	5	0.2	4	-4
DG2	19	0.5	0.08	0.4	-0.4
DG3	24	0.5	0.08	0.4	-0.4
DG4	33	0.5	0.08	0.4	-0.4
DG5	43	5	0.2	4	-4

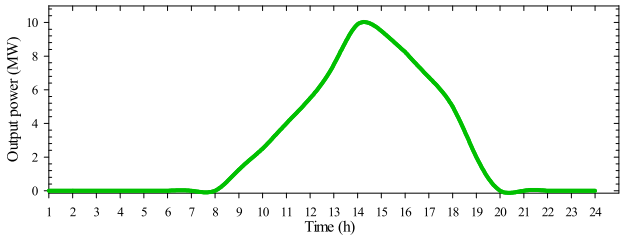

FIGURE 3. Active power of photovoltaic [45].

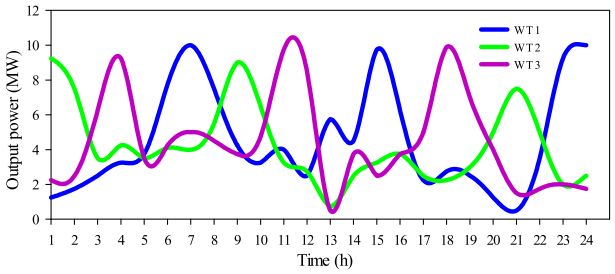

FIGURE 4. Active power of wind turbines [45].

incline to evacuate the cities, which can give rise to extensive traffic congestion for a long period of time like three days in some cases [46]. Therefore, in order to consider the traffic issues after the occurrence of the event and likely congestions, traffic congestion factor (TCF) is defined as an emergency condition traveling time over the normal condition traveling time. In this study, it is assumed that the value of TCF is set equal to two. It is also assumed that two crew teams are available in the system where a depot and two staging locations are considered as can be observed in Fig. 1.

To capture uncertainties associated with line damages caused by the event, 1000 random scenarios are firstly generated via the Monte Carlo simulation algorithm. Then, the SCENRED toolbox of the general algebraic modeling system (GAMS) is used to reduce the number of scenarios to 20 [47]. Table 2 provides reduced scenarios and their associated probabilities. Moreover, the data required for calculating the traveling time of crew teams between different

TABLE 2. Sample of the 20 reduced scenarios and their probabilities.

Scenario	Damaged lines	Probability
Sc.1	Lines 3-4, 18-19, 25-27, 30-31,35-36, 38-39, 43-44	0.043
Sc.2	Lines 3-4, 10-11, 18-19, 25-27, 30-31,35-36, 38-39, 43-44	0.094
Sc.5	Lines 3-4, 10-11, 18-19, 25-27, 30-31,35-36	0.024
…	…	…
Sc.17	Lines 3-4, 10-11, 13-14, 18-19, 25-27, 30-31, 35-36, 38-39, 43-44	0.1
Sc.18	Lines 3-4, 5-6, 8-9, 10-11, 13-14, 18-19, 1-22, 22-23, 25-27, 30-31,35-36, 43-44	0.06
Sc.20	Lines 3-4, 10-11, 18-19, 1-22, 25-27, 30-31,35-36, 43-44	0.041

TABLE 3. Traveling time between different points (lines, depot and staging locations) extracted from google maps (minutes).

From: to	Time	From: to	Time	From: to	Time
8-9:18-19	20	8-9:30-31	15	8-9:38-39	10
8-9:9-17	10	8-9:21-30	15	8-9:31-48	25
8-9: S1	10	8-9: S2	15	Depot:8-9	10
18-19:30-31	10	18-19:38-39	15	18-19:9-17	10
18-19:21-30	10	18-19:31-48	25	18-19: S1	5
18-19: S2	10	Depot:18-19	15	30-31:38-39	20
30-31:9-17	10	30-31:21-30	5	30-31:31-48	20
30-31: S1	15	30-31: S2	10	Depot:30-31	25
38-39:9-17	15	38-39:21-30	20	38-39:31-48	20
38-39: S1	15	38-39: S2	10	Depot:38-39	15
9-17:21-30	10	9-17: 31-48	20	9-17: S1	5
9-17: S2	10	Depot: 9-17	10	21-30: 31-48	10
21-30: S1	10	21-30: S2	15	Depot:21-30	20
31-48: S1	20	31-48: S2	15	Depot:31-48	30
S1: S2	10	Depot: S1	15	Depot; S2	20

points are given in Table 3, which are taken from Google Maps [48]. It is worthwhile to mention that the time required for changing the status of a switch is assumed to be 5 minutes. The simulations are executed on a PC with Intel Core i5 CPU @3.40 GHz and 8 GB RAM. The proposed model is solved in the GAMS environment with zero optimality gap. It should be noted that all of the simulations take less than the 3 minutes, which indicates the efficiency of the calculation.

TABLE 4. Actions taken by crew teams before the event.

Crews	Route and switching actions	Time (minutes)
Crew1	Depot → SW4 → SW1 → S2	15-30-40
Crew2	Depot → SW2 → S1	25-35
-	RCS1	40

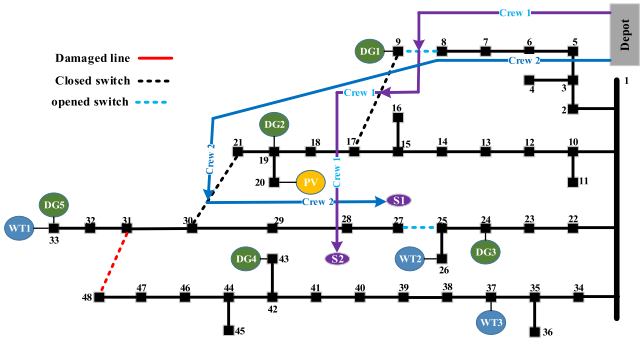

FIGURE 5. Pre-disturbance scheduling of two available crew teams.

To examine the performance of the proposed model, it is assumed that the approaching event is predicted 45 minutes before it hits the system. With this assumption, pre-disturbance scheduling of the crew teams after running the proposed model is given in Table 4. In addition, the schematic illustration of crew dispatching to the switch locations is shown in Fig. 5. As can be seen, as the first action, Crew 1 travels from depot location to the location of SW4 and then opens the switch with the total time of 15 minutes (i.e., 10 minutes for travel time and 5 minutes for changing

the status of the switch). After accomplishing this action, the crew moves to the location of SW1 in order to close the switch, which takes 30 minutes. Simultaneously, the second crew moves from depot to the location of SW2 to close it. This action takes 25 minutes. Crews 1 and 2 are then dispatched to the staging locations 2 and 1 prior to the approaching disaster, respectively. Finally, the switch of line 25-27 is opened remotely after 40 minutes. Needless to mention, these actions are taken considering the tough time limits (i.e., 45 minutes period).

A. CASE I

In this case, it is assumed that Scenario 5 happens after the occurrence of the event. This scenario is discussed since it is the best among all simulated scenarios. The line damages caused by the disturbance in this scenario are depicted in Fig. 6. Considering the damages, there are no required switching actions in the post-disturbance stage in this scenario. However, if the proactive actions are not employed, the actions itemized in Table 5 are required to be applied after the disturbance to restore the system. The actions are graphically depicted in Fig. 6 too. As can be seen, after the occurrence of the disturbance, in order to restore the curtailed loads, Crew 1 moves to the location of SW2 and closes it, which takes 45 minutes. Then, the crew moves toward the depot.

TABLE 5. Actions taken by crew teams after the event if no proactive action is performed: Case I.

Crews	Route and switching actions	Time (minutes)
Crew1	Depot → SW2 →Depot	45-85

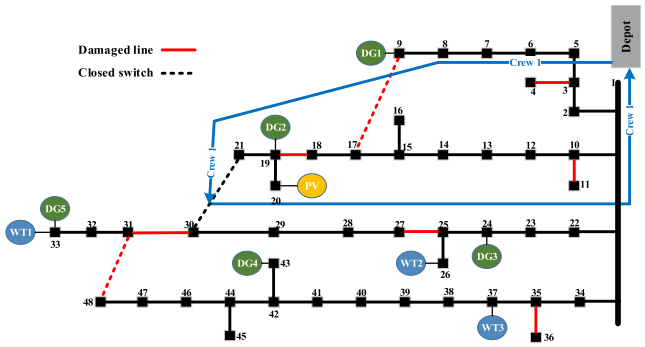

FIGURE 6. Post-disturbance scheduling of crew teams without proactive actions in case I.

Fig. 7 compares the amount of load curtailments during Scenario 1 for the two simulated situations with and without taking pre-disturbance actions. As can be seen, after the occurrence of the disturbance, supplied load level of the system falls down to 85% when the pre-disturbance actions are not applied. The level rises to 96.78% after 45 minutes. However, the total supplied load level falls down to 96.78% if the scheduled actions are applied before the disturbance

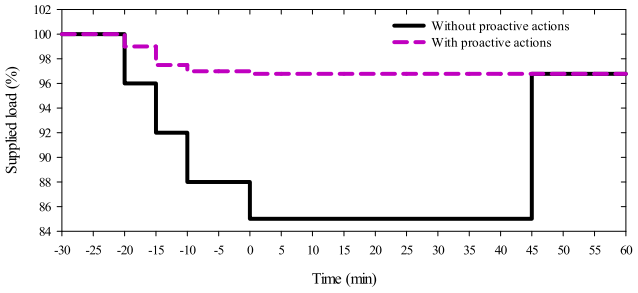

FIGURE 7. The restoration process of the system load in case I.

hits the system. In addition, the curtailed energy without taking the pre-disturbance scheduling is 3.105 MWh within the first hour after the disturbance. This index, in the presence of pre-disturbance scheduling, is equal to 1.08 MWh. This demonstrates the great potential of the proposed model in scheduling pre-disturbance actions. Hence, considering the acquired results, the proposed proactive scheduling approach has noticeably enhanced the resilience level of the system.

B. CASE II

In this case, it is assumed that Scenario 18 takes place. This scenario is discussed since it is the worst among all simulated scenarios. The line damages caused by the disturbance in this scenario are depicted in Fig. 8. Considering the damaged lines and pre-disturbance actions describe earlier, the actions given in Table 6 are required to be conducted after the disturbance. As can be observed in Fig. 8, applying the scheduled proactive actions, the crew teams require only one switching action to take. In this regard, Crew 1 moves from S2 to the location of SW3 and closes it within 35 minutes. Then, both of the crews move to the depot location. However, the crew teams have

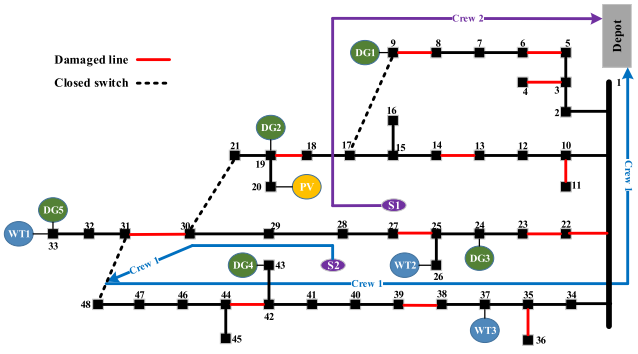

FIGURE 8. Post-disturbance scheduling of crew teams with proactive actions in case II.

TABLE 6. Actions taken by crew teams after the event if the proactive actions are performed: Case II.

Crews	Route and switching actions	Time (minutes)
Crew1	S2 → SW3 → Depot	35-95
Crew2	S1→ Depot	30

TABLE 7. Actions taken by crew teams after the event if no proactive action is performed: Case II.

Crews	Route and switching actions	Time (minutes)
Crew1	Depot → SW2→ SW3 → Depot	45-70-130
Crew2	Depot→ SW1→ Depot	35-65

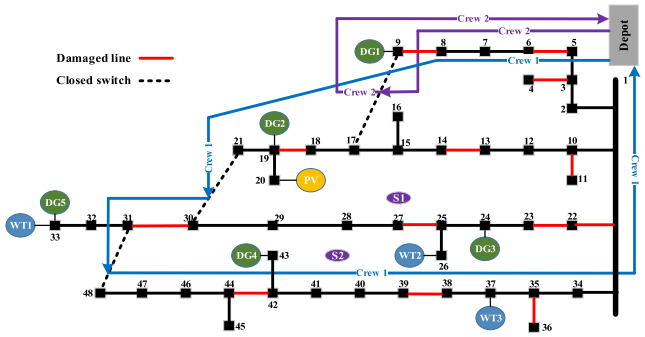

FIGURE 9. Post-disturbance scheduling of crew teams without proactive actions in case II.

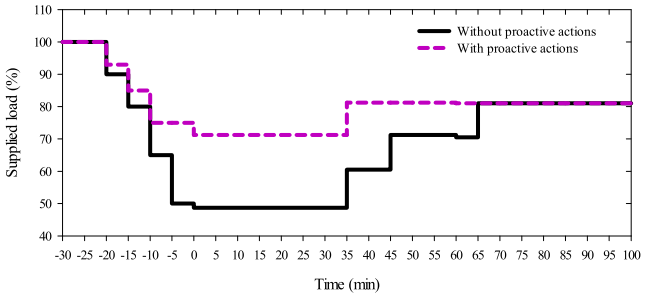

FIGURE 10. The restoration process of the system load in case II.

to take actions presented in Table 7 if no proactive action is considered. The actions are pictorially depicted in Fig. 9 as well. As can be seen, Crew 1 is dispatched from depot to the location of SW2, which takes 45 minutes. The crew is then dispatched to close SW3. This action takes 70 minutes. Meanwhile, the second crew is dispatched to the location of SW1 to close it, which takes 35 minutes. The profiles of load curtailments during Scenario 2 with and without taking pre-disturbance actions are compared in Fig. 10. As can be observed, in the presence of the pre-disturbance actions, the system experiences less interruptions compared to the situation where no proactive action is carried out. In addition, the total energy curtailment within two hours after the occurrence of the disturbance is equal to 16.217 if no proactive action is applied. This index is declined to 11.18 MWh if the scheduled proactive actions are performed. Therefore, implementing the proposed optimization scheme, the system operators not only have alleviated the initial load curtailment of the system but also recovered the system more quickly. Accordingly, the model mitigates the repercussions of the upcoming natural calamity effectively.

C. CASE III

In this case, Scenario 17 is considered for implementing sensitivity analyses on some key affecting parameters. This scenario is selected since it is the most likely scenario among all simulated scenarios. Table 8 presents the required post-disturbance actions if the scheduled pre-disturbance actions are performed. As can be seen, in this scenario, Crew 1 is dispatched to close SW3 first. It moves to the depot location thereafter. Since there is no additional action to do, Crew 2 directly moves to the depot location. Note that, in this case, after the event hits, 87.8% of the total load is supplied. The amount of supplied load rises to 96.8% after closing SW3.

TABLE 8. Actions taken by crew teams after the event if the proactive actions are performed: Case III.

Crews	Route	Time (minutes)
Crew1	S2 → SW3 → Depot	35-95
Crew2	S1 →Depot	30

In order to investigate the impact of key parameters on the performance of the proposed model, three sensitivity analyses are conducted here. Note that these analyses are conducted on Case III. At first, a sensitivity analysis is conducted to investigate the impact of the EP on the amount of curtailed load after the occurrence of the event. To do so, different values for EP are considered and actions taken by the crew teams before and after the disturbance are given in Table 9. In addition, the amount of supplied load after the disturbance hits is shown in Fig 11. As can be seen, predictability of the approaching event has a drastic impact on the amount of curtailed load in the system. It stands to reason that the system operator is able to better schedule the resources and take more actions as there is more time before the disturbance hits the system. As another observation, the amount of load at a particular moment after the event is not necessarily less for smaller EP values. This is mainly due to the different weight factors at different load points as well as the fact that the objective aims at minimizing the weighted energy interruption during the whole time. In summary, the amount of weighted energy interruption caused by the event decreases as the system operator has more time before the disturbance hits the system.

The impact of the number of available crew teams on the service restoration of the system is scrutinized here. The value of EP is set to 50 minutes in the analysis. The analysis is performed and the achieved results are provided in Table 10. It is worthwhile to note that the amount of curtailed energy provided in the table is calculated for the period until 2 hours after the disturbance. As can be seen, without exerting the proactive actions, altering the number of crew teams does not affect the amount of load survived after the occurrence of the disturbance. However, increasing the number of crew teams significantly declines the amount of curtailed energy in the system. On the other hand, implementing the proposed

TABLE 9. Crew actions before and after the event for different EP values.

EP (min)	Stage	Crews	Route	Time (min)
0	Pre-	Crew1	-	-
		Crew2	-	-
	Post-	Crew1	Depot → SW2 → SW3 → Depot	45-70-130
		Crew2	Depot → SW1 → Depot	35-65
15	Pre-	Crew1	Depot → S1	15
		Crew2	Depot → S1	15
	Post-	Crew1	S1 → SW1 → Depot	15-45
		Crew2	S1 → SW2→ SW3 → Depot	25-50-110
20	Pre-	Crew1	Depot → S1	15
		Crew2	Depot → S2	20
	Post-	Crew1	S1 → SW1 → SW2 → Depot	15-40-80
		Crew2	S2 → SW3 → Depot	35-95
30	Pre-	Crew1	Depot → SW1 → S1	20-25
		Crew2	Depot → SW4 → S2	15-30
	Post-	Crew1	S1 → SW2 → Depot	25-65
		Crew2	S2 → SW3 → Depot	35-95
35	Pre-	Crew1	Depot → SW2 → S1	25-35
		Crew2	Depot → SW7 → S2	20-30
	Post-	Crew1	S1 → SW1 → Depot	15-45
		Crew2	S2 → SW3 → Depot	35-95
40	Pre-	Crew1	Depot → SW4 → SW1 → S2	15-30-40
		Crew2	Depot → SW2 → S1	25-35
	Post-	Crew1	S2 → SW3 → Depot	35-95
		Crew2	S1 →Depot	30
50	Pre-	Crew1	Depot → SW2 → S1	25-35
		Crew2	Depot → SW3 → S2	35-50
	Post-	Crew1	S1 → SW1 → Depot	15-45
		Crew2	S2 → Depot	40
55	Pre-	Crew1	Depot → SW4 → SW1 → SW2 → S1	15-30-45-55
		Crew2	Depot → SW3 → S1	35-55
	Post-	Crew1	S1 → Depot	30
		Crew2	S1 → Depot	30

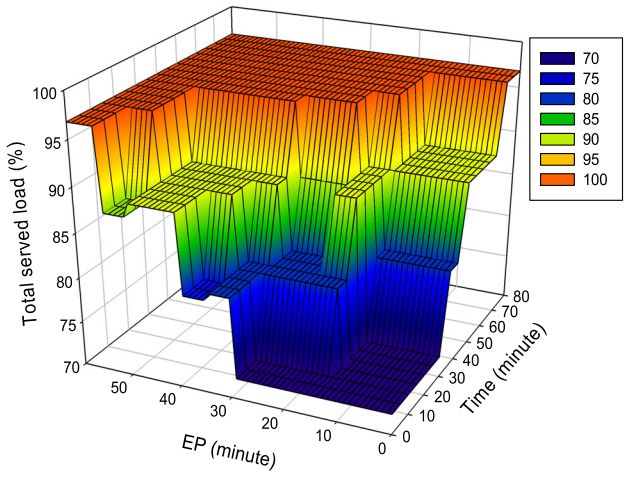

FIGURE 11. The restoration process of the system load after the event versus EP.

model to schedule proactive actions, by increasing the number of crew teams, the system operator not only acquires a more robust configuration which leads to more supplied load

TABLE 10. Impact of the number of crew teams on the initial load curtailment and restoration process of the system.

Strategy	Number of crews	Load served after the event (%)	Energy curtailment (MWh)
Without proactive actions	1	72.34	7.757
	2	72.34	6.759
	3	72.34	6.595
With proactive actions	1	79.84	3.631
	2	87.89	2.282
	3	96.78	1.721

level after the disturbance, but also, he/she can recover the system from the devastated state quickly, which gives rise to less energy curtailment and customer interruption.

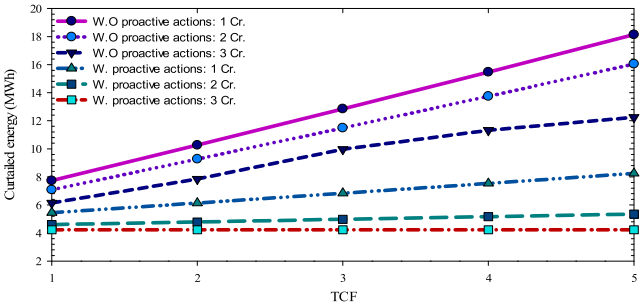

FIGURE 12. Curtailed energy of the system regarding the value of TCF and number of crew teams.

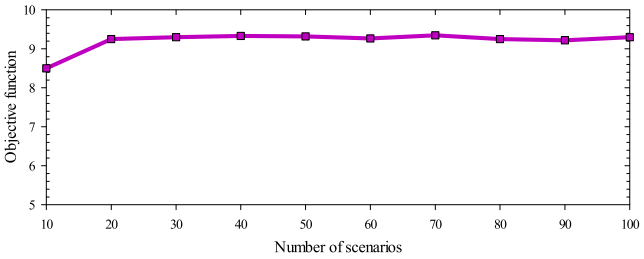

FIGURE 13. The value of the objective function versus the number of scenarios.

Also, another sensitivity analysis is conducted on the value of TCF in order to investigate the effect of traffic congestion on the restoration process after the disturbance hits. To do so, the amount of curtailed energy within 5 hours after the occurrence of the disturbance is calculated by increasing the value of TCF in both strategies (i.e., with and without proactive actions), while considering the different numbers of crew teams. As can be observed in Fig. 12, the value of TCF significantly affects the amount of curtailed energy. Especially, without implementing the proactive actions, since all the actions take place after the disturbance, increasing the TCF value has a drastic impact on the curtailed energy. Accordingly, in case a natural calamity induces a prevalent impact on the transportation system (e.g., floods), the importance and motivation of implementing the proposed model to schedule appropriate proactive actions are even more. Finally, to analyze whether the set of reduced scenarios is capable of covering the associated uncertainties, solution stability test is

applied to the problem. As can be seen in Fig. 13, regarding 20 scenarios, the solution is stable.

V. CONCLUSION

In this paper, a stochastic model was developed to enhance power distribution system resilience against predictable natural hazards. In the model, system resources are optimally scheduled in pre- and post-disturbance stages. In this model, the system is optimally reconfigured via taking advantage of available resources (e.g., DGs, WTs, and PVs), RCSs, and dispatching the crew teams to MS locations. The optimal placement of available crew teams in advance of the approaching disturbance is also considered in the model. To do so, the likely restoration processes of the system in the post-disturbance is simulated and a unique decision has been made. In order to capture the uncertain behavior of disturbances, several scenarios were sampled via Monte Carlo simulation technique for damage state of distribution lines. The scenarios are then reduced via SCENRED toolbox in GAMS to achieve a problem with affordable computational complexity. The performance of the proposed model was demonstrated by conducting different analyses on a typical distribution system. The achieved results indicate that predictability of the event and number of available crew teams have significant impacts on service restoration after the disastrous event hits the system.

REFERENCES

[1] Y. Wang, C. Chen, J. Wang, and R. Baldick, "Research on resilience of power systems under natural disasters—A review," *IEEE Trans. Power Syst.*, vol. 31, no. 2, pp. 1604–1613, Mar. 2015.
[2] A. Gholami, F. Aminifar, and M. Shahidehpour, "Front lines against the darkness: Enhancing the resilience of the electricity grid through microgrid facilities," *IEEE Electrific. Mag.*, vol. 4, no. 1, pp. 18–24, Mar. 2016.
[3] L. Che, M. Khodayar, and M. Shahidehpour, "Only connect: Microgrids for distribution system restoration," *IEEE Power Energy Mag.*, vol. 12, no. 1, pp. 70–81, Jan./Feb. 2014.
[4] R. Billinton, *Power System Reliability Evaluation*. New York, NY, USA: Taylor & Francis, 1970.
[5] A. Gholami, T. Shekari, M. H. Amirioun, F. Aminifar, M. H. Amini, and A. Sargolzaei, "Toward a consensus on the definition and taxonomy of power system resilience," *IEEE Access*, vol. 6, pp. 32035–32053, 2018.
[6] D. D. Woods, "Creating foresight: How resilience engineering can transform NASA's approach to risky decision making," *Work*, vol. 4, no. 2, pp. 137–144, Oct. 2003.
[7] M. Chaudry, P. Ekins, K. Ramachandran, A. Shakoor, J. Skea, G. Strbac, X. Wang, and J. Whitaker, "Building a resilient UK energy system," UK Energy Res. Centre, London, U.K., 2011. [Online]. Available: http://www.ukerc.ac.uk/publications/building-a-resilient-uk-energy-system-research-report.html
[8] A. R. Berkeley, M. Wallace, and C. Coo, "A framework for establishing critical infrastructure resilience goals," Nat. Infrastruct. Advisory Council, U.S. Dept. Homeland Secur., Washington, DC, USA, Final Rep., 2010. [Online]. Available: https://www.dhs.gov/xlibrary/assets/niac/niac-a-framework-for-establishing-critical-infrastructure-resilience-goals-2010-10-19.pdf
[9] *Presidential Policy Directive—Critical Infrastructure Security and Resilience|Whitehouse.Gov*. Accessed: Jan. 7, 2019. [Online]. Available: https://obamawhitehouse.archives.gov/the press-office/2013/02
[10] B. Cai, M. Xie, Y. Liu, Y. Liu, and Q. Feng, "Availability-based engineering resilience metric and its corresponding evaluation methodology," *Rel. Eng. Syst. Saf.*, vol. 172, pp. 216–224, Apr. 2018.
[11] M. Panteli, D. N. Trakas, P. Mancarella, and N. D. Hatziargyriou, "Power systems resilience assessment: Hardening and smart operational enhancement strategies," *Proc. IEEE*, vol. 105, no. 7, pp. 1202–1213, Jul. 2017.
[12] S. Ma, B. Chen, and Z. Wang, "Resilience enhancement strategy for distribution systems under extreme weather events," *IEEE Trans. Smart Grid*, vol. 9, no. 2, pp. 1442–1451, Mar. 2018.
[13] S. Ma, L. Su, Z. Wang, F. Qiu, and G. Guo, "Resilience enhancement of distribution grids against extreme weather events," *IEEE Trans. Power Syst.*, vol. 33, no. 5, pp. 4842–4853, Sep. 2018.
[14] R. T. Rockafellar and J.-B. Wets, "Scenarios and policy aggregation in optimization under uncertainty," *Math. Oper. Res.*, vol. 16, no. 1, pp. 119–147, Feb. 1991.
[15] J. P. Watson and D. L. Woodruff, "Progressive hedging innovations for a class of stochastic mixed-integer resource allocation problems," *Comput. Manage. Sci.*, vol. 8, no. 4, pp. 355–370, Nov. 2011.
[16] Q. Feng, X. Zhao, D. Fan, B. Cai, Y. Liu, and Y. Ren, "Resilience design method based on meta-structure: A case study of offshore wind farm," *Rel. Eng. Syst. Saf.*, vol. 186, pp. 232–244, Jun. 2019.
[17] Z. Wang and J. Wang, "Self-healing resilient distribution systems based on sectionalization into microgrids," *IEEE Trans. Power Syst.*, vol. 30, no. 6, pp. 3139–3149, Nov. 2015.
[18] Y. Liu, S. Lei, and Y. Hou, "Restoration of power distribution systems with multiple data centers as critical loads," *IEEE Trans. Smart Grid*, vol. 10, no. 5, pp. 5294–5307, Sep. 2018.
[19] C. Chen, J. Wang, F. Qiu, and D. Zhao, "Resilient distribution system by microgrids formation after natural disasters," *IEEE Trans. Smart Grid*, vol. 7, no. 2, pp. 958–966, Mar. 2016.
[20] B. Chen, C. Chen, J. Wang, and K. L. Butler-Purry, "Multi-time step service restoration for advanced distribution systems and microgrids," *IEEE Trans. Smart Grid*, vol. 9, no. 6, pp. 6793–6805, Nov. 2018.
[21] J. Kim and Y. Dvorkin, "Enhancing distribution system resilience with mobile energy storage and microgrids," *IEEE Trans. Smart Grid*, vol. 10, no. 5, pp. 4996–5006, Sep. 2018.
[22] Y. Ren, D. Fan, Q. Feng, Z. Wang, B. Sun, and D. Yang, "Agent-based restoration approach for reliability with load balancing on smart grids," *Appl. Energy*, vol. 249, pp. 46–57, Sep. 2019.
[23] A. Gholami, T. Shekari, and S. Grijalva, "Proactive management of microgrids for resiliency enhancement: An adaptive robust approach," *IEEE Trans. Sustain. Energy*, vol. 10, no. 1, pp. 470–480, Jan. 2017.
[24] M. Panteli, P. Mancarella, D. N. Trakas, E. Kyriakides, and N. D. Hatziargyriou, "Metrics and quantification of operational and infrastructure resilience in power systems," *IEEE Trans. Power Syst.*, vol. 32, no. 6, pp. 4732–4742, Nov. 2017.
[25] C. Wang, Y. Hou, F. Qiu, S. Lei, and K. Liu, "Resilience enhancement with sequentially proactive operation strategies," *IEEE Trans. Power Syst.*, vol. 32, no. 4, pp. 2847–2857, Jul. 2017.
[26] B. Taheri, A. Safdarian, M. Moeini-Aghtaie, and M. Lehtonen, "Distribution systems resilience enhancement via pre-and post-event actions," *IET Smart Grid*, to be published.
[27] S. Wang, B. R. Sarker, L. Mann, Jr., and E. Triantaphyllou, "Resource planning and a depot location model for electric power restoration," *Euro. J. Oper. Res.*, vol. 155, no. 1, pp. 22–43, May 2004.
[28] A. Arab, A. Khodaei, S. K. Khator, K. Ding, V. A. Emesih, and Z. Han, "Stochastic pre-hurricane restoration planning for electric power systems infrastructure," *IEEE Trans. Smart Grid*, vol. 6, no. 2, pp. 1046–1054, Mar. 2015.
[29] S. Lei, J. Wang, C. Chen, and Y. Hou, "Mobile emergency generator pre-positioning and real-time allocation for resilient response to natural disasters," *IEEE Trans. Smart Grid*, vol. 9, no. 3, pp. 2030–2041, May 2016.
[30] S. Lei, C. Chen, H. Zhou, and Y. Hou, "Routing and scheduling of mobile power sources for distribution system resilience enhancement," *IEEE Trans. Smart Grid*, vol. 10, no. 5, pp. 5650–5662, Sep. 2019.
[31] M. H. Amirioun, F. Aminifar, and H. Lesani, "Towards proactive scheduling of microgrids against extreme floods," *IEEE Trans. Smart Grid*, vol. 9, no. 4, pp. 3900–3902, Jul. 2018.
[32] M. H. Amirioun, F. Aminifar, and H. Lesani, "Resilience-oriented proactive management of microgrids against windstorms," *IEEE Trans. Power Syst.*, vol. 33, no. 4, pp. 4275–4284, Jul. 2018.
[33] A. Arif, Z. Wang, J. Wang, and C. Chen, "Power distribution system outage management with co-optimization of repairs, reconfiguration, and DG dispatch," *IEEE Trans. Smart Grid*, vol. 9, no. 5, pp. 4109–4118, Sep. 2018.
[34] A. Arif, S. Ma, Z. Wang, J. Wang, S. M. Ryan, and C. Chen, "Optimizing service restoration in distribution systems with uncertain repair time and demand," *IEEE Trans. Power Syst.*, vol. 33, no. 6, pp. 6828–6838, Nov. 2018.

[35] M. Panteli, C. Pickering, S. Wilkinson, R. Dawson, and P. Mancarella, "Power system resilience to extreme weather: Fragility modeling, probabilistic impact assessment, and adaptation measures," *IEEE Trans. Power Syst.*, vol. 32, no. 5, pp. 3747–3757, Sep. 2017.
[36] M. Panteli and P. Mancarella, "Modeling and evaluating the resilience of critical electrical power infrastructure to extreme weather events," *IEEE Syst. J.*, vol. 11, no. 3, pp. 1733–1742, Sep. 2017.
[37] B. Cai, X. Shao, Y. Liu, X. Kong, H. Wang, H. Xu, and W. Ge, "Remaining useful life estimation of structure systems under the influence of multiple causes: Subsea pipelines as a case study," *IEEE Trans. Ind. Electron.*, to be published.
[38] M. E. Baran and F. F. Wu, "Optimal capacitor placement on radial distribution systems," *IEEE Trans. Power Del.*, vol. 4, no. 1, pp. 725–734, Jan. 1989.
[39] Z. Wang, B. Chen, J. Wang, and J. Kim, "Decentralized energy management system for networked microgrids in grid-connected and islanded modes," *IEEE Trans. Smart Grid*, vol. 7, no. 2, pp. 1097–1105, Mar. 2016.
[40] S. Y. Derakhshandeh, A. S. Masoum, S. Deilami, M. A. S. Masoum, and M. E. Hamedani Golshan, "Coordination of Generation Scheduling with PEVs charging in industrial microgrids," *IEEE Trans. Power Syst.*, vol. 28, no. 3, pp. 3451–3461, Aug. 2013.
[41] M. R. Sarker, M. A. Ortega-Vazquez, and D. S. Kirschen, "Optimal coordination and scheduling of demand response via monetary incentives," *IEEE Trans. Smart Grid*, vol. 6, no. 3, pp. 1341–1352, May 2015.
[42] R. A. Jabr, R. Singh, and B. C. Pal, "Minimum loss network reconfiguration using mixed-integer convex programming," *IEEE Trans. Power Syst.*, vol. 27, no. 2, pp. 1106–1115, May 2012.
[43] B. A. McCarl, A. Meeraus, P. van der Eijk, M. Bussieck, S. Dirkse, P. Steacy, and F. Nelissen, "McCarl GAMS user guide," Version 24.0, GAMS Develop. Corp., Fairfax, VA, USA, 2014. [Online]. Available: http://citeseerx.ist.psu.edu/viewdoc/download?doi=10.1.1.296.8710&rep=rep1&type=pdf
[44] *The Branch and Bound Method*. Accessed: Aug. 7, 2019. [Online]. Available: http://compalg.inf.elte.hu/tony/Oktatas/SecondExpert/Chapter24-Branch6April.pdf
[45] M. Rahmani-Andebili and M. Fotuhi-Firuzabad, "An adaptive approach for PEVs charging management and reconfiguration of electrical distribution system penetrated by renewables," *IEEE Trans. Ind. Informat.*, vol. 14, no. 5, pp. 2001–2010, May 2018.
[46] *Will Another Traffic Nightmare Precede the Next Big Storm?|Road From Rita*. [Online]. Available: https://apps.texastribune.org/road-from-rita/taking-on-traffic/
[47] *SCENRED*. Accessed: Jan. 7, 2019. [Online]. Available: https://www.gams.com/latest/docs/T_SCENRED.html
[48] *Google Maps*. Accessed: Nov. 7, 2018. [Online]. Available: https://www.google.com/maps

BABAK TAHERI received the B.Sc. degree (Hons.) in electrical engineering from the University of Tabriz, Tabriz, Iran, in 2017, and the M.Sc. degree (Hons.) in electrical engineering from the Sharif University of Technology, Tehran, Iran, in 2019. His current research interests include power system operation and planning, smart grid issues, power system optimization, power system resilience and reliability, renewable energies, electricity markets, and power system economics.

AMIR SAFDARIAN received the B.Sc. degree from Tehran University, Tehran, Iran, in 2008, and the M.Sc. and Ph.D. degrees from the Sharif University of Technology, Tehran, Iran, in 2010 and 2014, respectively, where he is currently an Assistant Professor. His current research interests include distribution system operation and planning, smart grid issues, and power system reliability and resilience. He was a recipient of the 2013 IEEE Power System Operation Transactions Prize Paper Award, the 2016 IEEE Iran Section Best Ph.D. Dissertation Award, and the 2019 IEEE Iran Section Young Investigator Award, and in the list of outstanding reviewers of the IEEE TRANSACTIONS ON SUSTAINABLE ENERGY, in 2016.

MOEIN MOEINI-AGHTAIE received the M.Sc. and Ph.D. degrees in electrical engineering from the Sharif University of Technology, Tehran, Iran, in 2010 and 2014, respectively, where he is currently an Assistant Professor with the Department of Energy Engineering. His current research interests include reliability and resilience studies of modern distribution systems, especially, in the multi-carrier energy environment and charging management of plug-in hybrid electric vehicles.

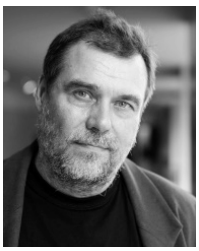

MATTI LEHTONEN received the M.S. and Licentiate degrees in electrical engineering from Aalto University (formerly, Helsinki University of Technology), Espoo, Finland, in 1984 and 1989, respectively, and the D.Sc. degree in electrical engineering from the Tampere University of Technology, Tampere, Finland, in 1992. Since 1987, he has been with VTT Energy, Espoo, and since 1999, he has been with the Department of Electrical Engineering and Automation, Aalto University, where he is currently a Professor of IT applications in power systems. His current research interests include earth fault problems and harmonic-related issues, and applications of information technology in distribution automation and distribution energy management.